



The Thermal Impact of THz Signaling in Protein Nanonetworks

Hadeel Elayan
Department of Electrical and
Computer Engineering
University of Toronto
Ontario, Canada

Samar Elmaadawy
Department of Electrical and
Computer Engineering
Northeastern University
Boston, United States

Andrew W. Eckford
Department of Electrical Engineering
and Computer Science
York University
Ontario, Canada

Raviraj Adve
Department of Electrical and
Computer Engineering
University of Toronto
Ontario, Canada

Josep Jornet
Department of Electrical and
Computer Engineering
Northeastern University
Boston, United States

ABSTRACT

Technological advancements in the terahertz (THz) frequency band have resulted in a surge of interest in the fundamental research as well as the practical applications of THz waves in the biomedical domain. In specific, the energy levels of protein vibrations coincide with those of THz waves, which increases the probability of their interaction. Nonetheless, one open research topic in this field involves understanding the thermal effect of THz radiation on protein networks, particularly under resonant conditions. In this work, we adopt the Goldenberg and Tranter heat diffusion model to study the thermal interaction between THz waves and protein molecules. We show that using different THz power levels results in various implications on protein interactions. In addition, we demonstrate the impact of resonance on protein absorption and the fundamental role it plays in increasing the temperature in protein networks. Finally, we numerically verify the analytical framework by building a physical model that mimics the THz-protein interaction using COMSOL Multiphysics®.

CCS CONCEPTS

• **Computing methodologies** → **Model verification and validation.**

KEYWORDS

Terahertz signaling, protein interactions, thermal effects.

ACM Reference Format:

Hadeel Elayan, Samar Elmaadawy, Andrew W. Eckford, Raviraj Adve, and Josep Jornet. 2023. The Thermal Impact of THz Signaling in Protein Nanonetworks. In *10th ACM International Conference on Nanoscale Computing and Communication (NANOCOM '23)*, September 20–22, 2023, Coventry, United Kingdom. ACM, New York, NY, USA, 6 pages. <https://doi.org/10.1145/3576781.3608730>

Permission to make digital or hard copies of all or part of this work for personal or classroom use is granted without fee provided that copies are not made or distributed for profit or commercial advantage and that copies bear this notice and the full citation on the first page. Copyrights for components of this work owned by others than the author(s) must be honored. Abstracting with credit is permitted. To copy otherwise, or republish, to post on servers or to redistribute to lists, requires prior specific permission and/or a fee. Request permissions from permissions@acm.org.
NANOCOM '23, September 20–22, 2023, Coventry, United Kingdom
© 2023 Copyright held by the owner/author(s). Publication rights licensed to ACM.
ACM ISBN 979-8-4007-0034-7/23/09...\$15.00
<https://doi.org/10.1145/3576781.3608730>

To establish feasible communication at the nanoscale, both molecular and electromagnetic (EM) communication paradigms have been introduced as potential solutions. Molecular communication (MC) involves encoding information into molecules and exchanging them via chemical signaling between either biological or engineered nanodevices [19]. Due to its potential, MC has been extensively studied over the past decade. Problems related to the capacity of the communication link, the development of appropriate modulation and coding techniques, as well as the proposal of networking protocols to optimize the transfer of information conveyed by molecules, have been considered.

In addition, from an EM perspective, the technological progress in the Terahertz (THz) frequency band, defined between 0.1 to 10 THz, has enabled new methods for controlling matter at the nanoscale [10]. The study of the biological effects of THz waves has become a prominent area of research due to the sensing abilities as well as the non-invasive and non-ionizing nature of THz frequencies [24]. For this reason, numerous research efforts have been targeting THz-EM communication with work spanning channel models, multi-layer propagation, as well as noise sources [4, 5].

However, to have an end-to-end model, we must bridge the gap between EM-nanocommunication and MC, as this will facilitate the development of feasible bio-nano-interfaces in a body area network. To address this challenge, we proposed in [2] a hybrid model based on protein signaling. On the one hand, proteins are natural communication agents that can be used to transmit information between nanoscale devices in a biocompatible and efficient manner. On the other hand, an important feature of protein molecules is the sensitivity of their vibrational modes to frequencies in the THz range [12]. THz vibrations have been observed in protein-ligand binding [27] and other biological polymers [30], suggesting that protein-ligand interactions trigger unique changes in vibration that can be used in detection and diagnoses. By understanding these collective modes, we can have insights into protein function and dynamics.

Although our proposed hybrid system has great potential, the heating effects of THz waves on intra-body nanonetworks remain an open research area. Heat transfer in the THz frequency range and its specific impact on proteins require a thorough understanding of heat transport mechanisms along with appropriate mathematical modeling. In fact, the previous photothermal models have been

limited to the cellular [3] and tissue level [21], where the assumption of a homogeneous medium dominates.

Further research is therefore needed to explore the potential applications of THz radiation in modulating protein functions for biomedical purposes. In this work, we theoretically calculate the temperature change experienced by protein particles under THz-EM wave illumination using the Goldenberg and Tranter [8] heat transfer model. We assume uniformly heated spherical proteins embedded in cytoplasm to mimic a biological environment. We also carry out numerical simulations via COMSOL Multiphysics® to complement the analytical framework.

The rest of the paper is organized as follows. In Sec. 1, we present the physical basis of the protein thermal process, where we introduce the concept of resonance absorption. In Sec. 2, we utilize the Goldenberg and Tranter heat transfer model to study the impact of the THz-induced thermal effects on protein molecules. We also explain the implications of the different THz power levels on protein interactions. In Sec. 3, we demonstrate our analytical and numerical results based on the developed models. Finally, we draw our conclusions in Sec. 4.

1 PHYSICAL BASIS

Resonant absorption is a phenomenon that occurs when a protein molecule absorbs EM radiation with a frequency that matches the excitation of electrons in the protein, causing them to move to higher energy levels. As a consequence, the protein's properties and structure may get altered [18]. When a protein molecule vibrates, it interacts with its surroundings, including the surrounding water molecules. These interactions cause the vibrational energy of the protein to gradually dissipate and convert to heat energy, which is then transferred to the environment.

It is to be noted that the rate at which the vibrational energy is converted into heat depends on several factors, including the size and shape of the protein molecule, as well as the nature of its surrounding environment. In general, larger proteins tend to have more vibrational modes and thus dissipate their energy more slowly than smaller proteins [15].

To understand protein resonant interactions and their relation to absorption, we need to examine the protein permittivity expressed as, $\epsilon_p(\omega) = \epsilon_p'(\omega) - j\epsilon_p''(\omega)$. The permittivity has its real part given by [12]

$$\epsilon_p'(\omega) = \epsilon_\infty + \frac{\epsilon_0 - \epsilon_\infty}{1 + (\omega\tau)^2} + \frac{(\epsilon_1 - \epsilon_\infty) \left[1 - \left(\frac{\omega}{\omega_0} \right)^2 \right]}{\left[1 - \left(\frac{\omega}{\omega_0} \right)^2 \right]^2 + (\omega\beta)^2}, \quad (1)$$

while the imaginary part yields

$$\epsilon_p''(\omega) = \frac{(\epsilon_0 - \epsilon_\infty)\omega\tau}{1 + (\omega\tau)^2} + \frac{(\epsilon_1 - \epsilon_\infty)\omega\beta}{\left[1 - \left(\frac{\omega}{\omega_0} \right)^2 \right]^2 + (\omega\beta)^2}. \quad (2)$$

Here, ϵ_0 is the permittivity at the low frequency limit (static regions), ω_0 is the natural frequency of the protein, and β is the damping constant, which governs the magnitude of the protein

Table 1: System Components

External Stimulus	Local Stimulus	Brain Interface	Nanotransducer
THz-EM signal	Heat	Temperature-gated ion channels	Protein Vibrational Modes

resonances. According to structural mechanics, if an external harmonic excitation, ω , has a frequency which matches one of the natural frequencies of the system, ω_0 , then resonance occurs, and the vibrational amplitude of the protein increases.

Next, we relate the permittivity to the complex refractive index $n(\omega)$ using

$$\epsilon_p(\omega) = n^2(\omega) = (n'(\omega) + jn''(\omega))^2. \quad (3)$$

In (3), $n'(\omega)$ and $n''(\omega)$ represent the refractive index real and imaginary parts, respectively. The real part of the refractive index, which expresses the phase velocity, is given as

$$n'(\omega) = \sqrt{\frac{1}{2} (|\epsilon_p(\omega)| + \epsilon_p'(\omega))}. \quad (4)$$

The imaginary part of the refractive index, which indicates the attenuation of the EM wave, is

$$n''(\omega) = \sqrt{\frac{1}{2} (|\epsilon_p(\omega)| - \epsilon_p'(\omega))}. \quad (5)$$

Here, $|\epsilon_p(\omega)|$ is the complex modulus given as $\sqrt{\epsilon_p'^2 + \epsilon_p''^2}$. Finally, from the refractive index, the protein absorption coefficient, C_{abs} , can be calculated using

$$C_{abs}(\omega) = \frac{4\pi n''(\omega)}{\lambda_g}, \quad (6)$$

where λ_g , the effective wavelength, is $\lambda/n'(\omega)$.

Table 1 explains the mechanism of THz-protein interactions and one of its possible applications. In fact, we consider the THz-EM signal as an external stimulus, which gets converted into heat due to the resonant absorption that occurs subsequent to the interaction between THz waves and the protein vibrational modes. As a result of the generated heat, the change in temperature can impact temperature-gated ion channels, which serve as an important component of neuronal signaling. Temperature-gated ion channels allow ions such as calcium or sodium to flow into or out of the cell. This can lead to changes in the neuron's membrane potential, which in turn affect its activity and ultimately contribute to the processing of information in the brain [13].

2 HEAT TRANSFER MODEL

Transportation of heat at the nanoscale is essentially distinct from that at larger scales, and it depends on how energy is dispersed in a substance, the dimensions of the heat sources, and the extent of the distance covered by the heat transfer [9].

The heat transfer model used in this work is based on spherical protein particles immersed in an aqueous medium, resembling the cytoplasm in the cell. Upon being triggered by a THz-EM signal, protein particles can be treated as heat sources.

While proteins and nanoparticles are fundamentally different in their composition, they do reveal similarities in their overall size, charge, and shape. As such, in our work, we adopt the Goldenberg

and Tranter model, which has been used to study heat transfer mechanisms experienced by nanoparticles [8, 11, 29]. We specifically deploy this model as it provides the time-dependent solution to the heat conduction problem involving a heated sphere situated within a medium with distinct thermal characteristics.

For one-dimensional transient heat transfer in spherical coordinate systems, we have

$$\frac{1}{\alpha_p} \frac{\partial T_p(r, t)}{\partial t} = \frac{1}{r^2} \frac{\partial}{\partial r} \left(r^2 \frac{\partial T_p}{\partial r} \right) + \frac{Q_v}{k_p} \quad (7)$$

$$\frac{1}{\alpha_m} \frac{\partial T_m(r, t)}{\partial t} = \frac{1}{r^2} \frac{\partial}{\partial r} \left(r^2 \frac{\partial T_m}{\partial r} \right), \quad (8)$$

where T is the temperature, k is the thermal conductivity and α is the thermal diffusivity. The subscripts m and p indicate the medium and the protein, respectively. In addition, r refers to the position and t is time. The energy transfer is uniform in the protein and can be considered as a uniform volumetric heating, Q_v , expressed by

$$Q_v = \frac{C_{abs} I}{v_p}. \quad (9)$$

Here, I is the nano-laser power density and v_p is the volume of the protein. In addition, the boundary and initial conditions are given as [11]

$$\begin{aligned} \frac{\partial T}{\partial r} \Big|_{r=0} &= 0, \\ T \Big|_{r=\infty} &= T_{ref} = 37^\circ \text{C}, \\ T \Big|_{t=0} &= T_{ref} = 37^\circ \text{C}. \end{aligned} \quad (10)$$

We neglect the thermal resistance at the interface between the protein and the medium since the conducting path for heat transfer is significantly longer compared to the inter-facial region. As such, the thermal resistance introduced by the interface becomes relatively small. This will result in the same temperature for the protein and the water immediately next to the protein surface. The continuous inter-facial conditions are described by the following equations [11]

$$\begin{aligned} T_p \Big|_{r=R_p^-} &= T_m \Big|_{r=R_p^+}, \\ k_p \frac{\partial T_p}{\partial r} \Big|_{r=R_p^-} &= k_m \frac{\partial T_m}{\partial r} \Big|_{r=R_p^+}, \end{aligned} \quad (11)$$

where R_p is the protein radius. Finally, the form of the analytical solutions of (7) and (8) are given by (12) and (13). Basically, (12) and (13) give the time-dependent temperature for an unlimited long pulse.

Since the differential equations for heat diffusion are linear in time, a solution for a rectangular laser pulse can be constructed by subtracting the two solutions $T(t, r)$, which are separated in time [17]

$$\Delta T = T(r, t) - T(r, t - \tau), \quad (14)$$

where τ is the pulse duration. Here, we focus on pulsed-laser illumination since given a fixed power density, we can regulate the increase in temperature by controlling the pulse width. On the contrary, when dealing with continuous-wave illumination, the only factor that can be managed is the laser power density. As such, through careful design of pulsed-illumination systems, we

can achieve the desired temperature increase to serve the intended biomedical purposes.

For a distribution of proteins, the temperature profile can be found using the superposition of the solution for single protein heating as follows [29]

$$T_{MP}(r, t) = \sum_{i=1}^N T_p^i(r^i, t), \quad (15)$$

where T_{MP} is the temperature profile for multiple particle heating and T_p^i is the analytical solution for the i^{th} single-particle heating given in (12).

Due to the dynamic nature of proteins, exposure to various THz-EM power levels, impact protein interactions differently. In this work, we distinguish between the implications of the radiation of three power levels: low, medium and high. We define a *low power THz-EM interaction* as one that does not induce any thermal effect on protein particles, where any temperature increase is less than 1°C .

When human cells are exposed to sudden environmental changes, they react by releasing molecular chaperones called heat shock proteins (HSP). The main role of HSPs is to guide proteins while folding, trafficking, unfolding, and refolding after being misfolded to preserve their physiological function. Therefore, HSPs protect the cell against heat or any other environmental stress [16].

Since the exposure to EM waves is considered a form of environmental stress, the detection of HSPs in cells should be possible even if there is no thermal impact. In fact, exposure to low power radiation at 60.4 GHz and 0.5 THz did not show any changes in the molecular level of protein structures as given in [20] and [23].

In addition, we define a *medium power THz-EM interaction* as one that modulates the activity of protein receptors by promoting conformational changes that allow the receptor to interact with other signaling molecules. Here, the expected temperature increase is between 1°C - 3°C [25]. For instance, a unique group of temperature-sensitive ion channels, named thermo-sensitive TRP channels has been recognized as primary bio-thermometers in a range of species. These receptors activate specific intra-cellular signaling pathways that can lead to changes in gene expression, cell proliferation, or other cellular processes [13].

Finally, we define a *high power THz-EM interaction* as one that cause thermal denaturation of proteins. In this scenario, the expected temperature increase is $\geq 4^\circ \text{C}$ [14]. Such temperature increase results in altering the secondary and tertiary structure of proteins, including disruption of hydrogen bonds, changes in the orientation of alpha-helices and beta-sheets, as well as changes in the solvent-accessible surface area of the protein [28]. Denaturation involves the disruption of the protein's native three-dimensional structure, thereby its active sites may be obscured, rendering it unable to carry out its specific biological functions.

3 RESULTS

The theoretical model presented in this work is validated using both MATLAB and COMSOL Multiphysics[®], where the simulation parameters are given in Table 2. In our model, we assume protein particles distributed on the surface of a cell and embedded in aqueous solution mimicking the cell cytoplasm. We perform the

$$T_p(r, t)|_{t < \tau} = T_{ref} + \frac{R_p^3 C_{abs} I}{k_p v_p} \left\{ \frac{k_p}{3k_m} + \frac{1}{6} \left(1 - \frac{r^2}{R_p^2} \right) - \frac{2R_p b}{r\pi} \int_0^\infty \frac{\exp\left(\frac{-y^2 t}{\gamma_1}\right)}{y^2} \frac{(\sin y - y \cos y) \sin\left(\frac{ry}{R_p}\right)}{[(c \sin y - y \cos y)^2 + b^2 y^2 \sin^2 y]} dy \right\}. \quad (12)$$

$$T_m(r, t)|_{t < \tau} = T_{ref} + \frac{R_p^3 C_{abs} I}{rk_p v_p} \left\{ \frac{k_p}{3k_m} - \frac{2}{\pi} \int_0^\infty \frac{\exp\left(\frac{-y^2 t}{\gamma_1}\right)}{y^3} \frac{(\sin y - y \cos y) [(by \sin y \cos \sigma y) - (c \sin y - y \cos y) \sin \sigma y]}{[(c \sin y - y \cos y)^2 + b^2 y^2 \sin^2 y]} dy \right\}. \quad (13)$$

$$b = \frac{k_m}{k_p} \sqrt{\frac{\alpha_p}{\alpha_m}}, c = 1 - \frac{k_m}{k_p}, \gamma_1 = \frac{R_p^2}{\alpha_p}, \sigma = \left(\frac{r}{R_p} - 1 \right) \sqrt{\frac{\alpha_p}{\alpha_m}}.$$

Table 2: Simulation Parameters

Parameter	Value	Ref
Protein Thermal Conductivity	0.1-0.2 W/m·K	[15]
Water Thermal Conductivity	0.6 W/m·K	[15]
Protein Specific Heat Capacity	1483 J/kg·K	[31]
Protein Density	1350 kg/m ³	[7]
Protein radius	5 nm	[6]
Inter-particle distance	10 nm	[6]
Number of particles	10 ⁴	-

Table 3: Protein Permittivity Values [26]

Protein Type	ϵ_∞	ϵ_o	ϵ_1	τ (ps)	ω_o (THz)	β (ps)
Lysozyme	1	216	0.73	400	1.8	0.02

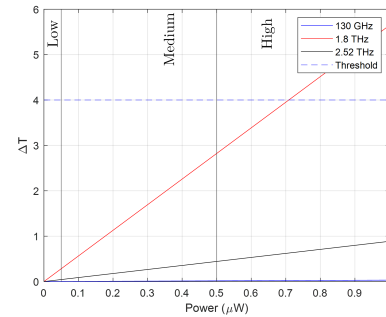
simulations on the protein lysozyme as all it needed parameters are provided in the literature as given in Table 3. For the cytoplasm, we use the parameters of water at THz provided in [22]. As explained in Sec.2, for all our simulations, we consider a group of protein particles. For THz induced temperature to impact protein molecules, the accumulation of heat fluxes produced by individual particles is required to create a measurable, cumulative temperature effect.

For the MATLAB results, we numerically evaluate (12), (13) and (15). We generate random positions for the protein particles over the surface of a single cell having an area of $10 \mu\text{m} \times 10 \mu\text{m}$. We also allocate a protein particle in the center to be our point of reference. The distance from the center of the reference particle to the boundary of the area is $5 \mu\text{m}$. We compute the temperature change based on the distance between the reference protein and the other proteins in the system.

Fig. 1 demonstrates the temperature increase versus the induced nano-laser beam power. The chosen simulation power range varies from nano-watts to micro-watts in order for us to be capable of visualizing the impact of low, medium and high-radiation power on temperature. Here, we set the pulse duration to 1 millisecond. We note that thermal denaturation of proteins occurs when the temperature increase is $\geq 4^\circ\text{C}$ [14]. Hence, this value represents a threshold that should not be exceeded for temperature increase.

It is noteworthy to indicate that Fig. 1 compares frequencies that include the widely used 130 GHz for wireless communication in the THz frequency band, the resonant frequency of protein lysozyme at 1.8 THz, and the conventional 2.52 THz frequency employed in THz imaging applications. At the resonant frequency of the protein lysozyme, we achieve the highest temperature increase. This result confirms the impact of the resonance absorption phenomenon and its role in converting protein particles into heating nanosources.

This effect is clearly present in Fig. 2a, which shows the temperature increase versus the nano-laser frequency for low and medium power levels. Further, in Fig. 2b, we demonstrate the temperature change associated with pulse durations in the millisecond range. In particular, for medium THz power radiation, a millisecond pulse is required to activate voltage-gated ion channels and trigger neuronal action potentials since the pulse duration must match the kinetic rate of the interaction [1].


Figure 1: Temperature increase versus power.

However, for certain applications, our aim would be to induce localized high temperature changes. For these scenarios, devices that operate in the micro-watt range are required. In fact, the exposure of mammalian cells to temperature ranges between $41-45^\circ\text{C}$ for short periods of time (referred to hyper-thermia) is sufficient to switch off protein activity in a living cell (unfold and inactivate targeted proteins) [14]. For these scenarios, we require short pulses to trigger a rapid diffusion of heat, resulting in localized

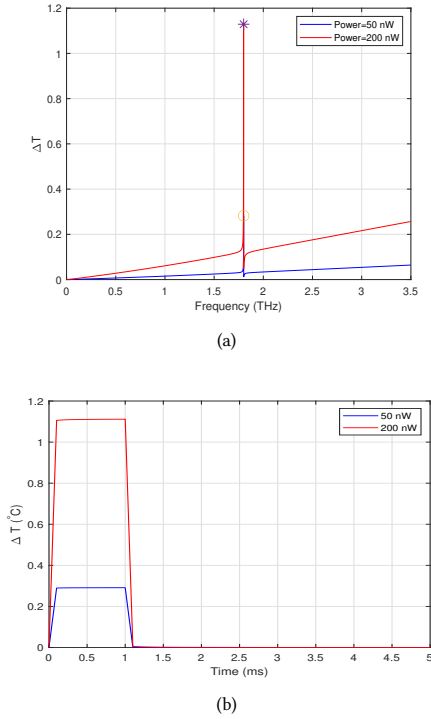


Figure 2: (a) Temperature increase versus frequency for low and medium THz radiation power levels. (The asterisk and circle indicate the highest temperature for each power level) (b) Temperature increase versus pulse width duration in the millisecond range.

heating [29]. Fig. 3a illustrates the capability to create high temperature changes in proteins when targeting them at their resonant frequencies. Nonetheless, the pulse widths for these applications should be short enough in order not to create macroscale heating in the system and impact untargeted regions. For these scenarios, the pulse width is restricted to the nanosecond timescale as presented in Fig. 3b. We notice from the figure how the temperature rises quickly and returns to its initial temperature at around 400 nanoseconds.

3.1 COMSOL Model

COMSOL Multiphysics[®] is used to verify the analytical model, where a physical system that captures the thermal effect of a 1.8 THz EM wave on a protein patch is presented. Specifically, we built a 2D parametric model of a $10 \mu\text{m} \times 10 \mu\text{m}$ patch of proteins embedded in cytoplasm (modelled as water). The size of the patch mimics the size of a single cell with protein particles distributed on the surface of the cell, similar to the MATLAB simulation setup. In addition, the protein patch is surrounded by an infinite element domain.

The COMSOL model is composed of two domains, one for the water and one for the protein. Each domain has its own set of thermal and electrical parameters as given in Tables 2 and 3. The source of radiation is a rectangular beam incident on the Dirichlet

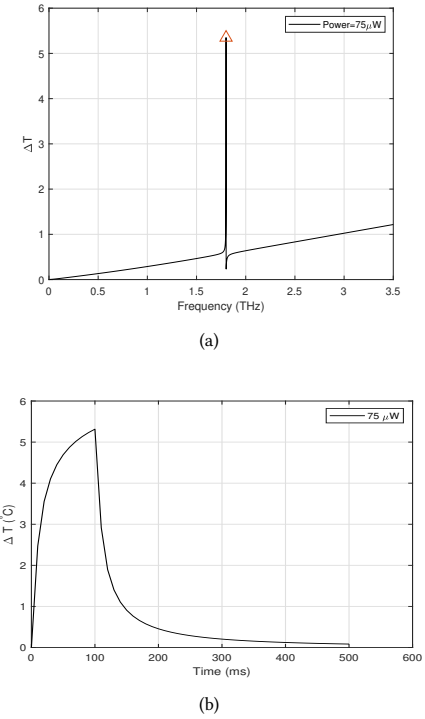


Figure 3: (a) Temperature increase versus frequency for a high THz radiation power level. (The triangle indicates the highest temperature for each power level) (b) Temperature increase versus pulse width duration in the nanosecond range.

boundary. It is to be noted that the same values used in the MATLAB simulation are used in the COMSOL model. In addition, the same surface area covered by the proteins in MATLAB is covered by the proteins in COMSOL.

Fig. 4 presents the interaction of a THz laser beam with a group of lysozyme proteins. The results clearly distinguish three regions of interactions: high power-short pulse, medium power-medium pulse, low power-long pulse. Specifically, Fig. 4(a) demonstrates a localized increase in temperature, where heat is applied to a small, specific region of the system. On the contrary, Fig. 4(b) shows macroscale heating, where heat is applied to a larger region resulting in a more uniform increase in temperature. This is due to the lower power and longer pulse duration in comparison to Fig. 4(b). Finally, when using low power radiation, we do not notice any thermal impact on the protein particles as illustrated in Fig. 4(c).

4 CONCLUSIONS

The thermal effects of THz radiation on proteins depend on several factors, including the power and frequency of the radiation, the composition and structure of the protein, and the surrounding environment. Nonetheless, the precise mechanisms underlying these effects are still not fully understood. In this paper, we use the Goldenberg and Tranter heat diffusion model to examine how THz waves interact with protein molecules. By varying the power levels,

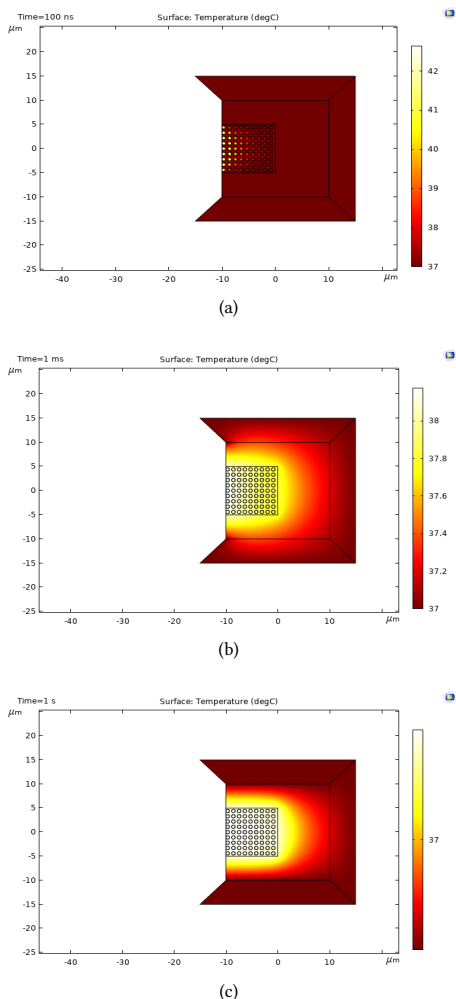


Figure 4: (a) Protein patch targeted using (a) 75 μ W laser beam for 100 nanoseconds (b) 200 nW laser beam for 1 millisecond (c) 50 nW laser beam for 1 second.

we found that protein interactions are affected differently by low, medium, and high power THz radiation. In addition, we showed how the combination of different pulse durations and power levels can have various implications on how to control THz induced protein interactions. We also highlighted the significance of resonance in increasing the temperature in protein networks as it is tied to the protein absorption characteristics. To verify the analytical framework, we built a physical model using COMSOL Multiphysics®. Our results indicate how THz-EM waves can be used as a controlling tool and a thermal-based technique for predicting how proteins interact with their environment under different thermal conditions.

REFERENCES

[1] B. Alberts, A. Johnson, J. Lewis, M. Raff, K. Roberts, and P. Walter. Ion channels and the electrical properties of membranes. In *Molecular Biology of the Cell. 4th edition*. Garland Science, 2002.

[2] H. Elayan, A. W. Eckford, and R. S. Adve. Information rates of controlled protein interactions using terahertz communication. *IEEE Transactions on NanoBioscience*, 20(1):9–19, 2020.

[3] H. Elayan, P. Johari, R. M. Shubair, and J. M. Jornet. Photothermal modeling and analysis of intrabody terahertz nanoscale communication. *IEEE Transactions on Nanobioscience*, 16(8):755–763, 2017.

[4] H. Elayan, R. M. Shubair, J. M. Jornet, and P. Johari. Terahertz channel model and link budget analysis for intrabody nanoscale communication. *IEEE Transactions on Nanobioscience*, 16(6):491–503, 2017.

[5] H. Elayan, C. Stefanini, R. M. Shubair, and J. M. Jornet. End-to-end noise model for intra-body terahertz nanoscale communication. *IEEE Transactions on Nanobioscience*, 17(4):464–473, 2018.

[6] H. P. Erickson. Size and shape of protein molecules at the nanometer level determined by sedimentation, gel filtration, and electron microscopy. *Biological procedures online*, 11:32–51, 2009.

[7] H. Fischer, I. Polikarpov, and A. F. Craievich. Average protein density is a molecular-weight-dependent function. *Protein Science*, 13(10):2825–2828, 2004.

[8] H. Goldenberg and C. Tranter. Heat flow in an infinite medium heated by a sphere. *British journal of applied physics*, 3(9):296, 1952.

[9] K. M. Hoogeboom-Pot et al. A new regime of nanoscale thermal transport: Collective diffusion increases dissipation efficiency. *Proceedings of the National Academy of Sciences*, 112(16):4846–4851, 2015.

[10] J. M. Jornet and I. F. Akyildiz. Graphene-based plasmonic nano-antenna for terahertz band communication in nanonetworks. *IEEE Journal on selected areas in communications*, 31(12):685–694, 2013.

[11] P. Kang et al. Computational investigation of protein photoinactivation by molecular hyperthermia. *Journal of biomechanical engineering*, 143(3), 2021.

[12] J. Knab, J.-Y. Chen, and A. Markelz. Hydration dependence of conformational dielectric relaxation of lysozyme. *Biophysical journal*, 90(7):2576–2581, 2006.

[13] J. A. Lamas, L. Rueda-Ruzafa, and S. Herrera-Pérez. Ion channels and thermosensitivity: TRP, TREK, or both? *International journal of molecular sciences*, 20(10):2371, 2019.

[14] J. R. Lepock, H. E. Frey, and K. P. Ritchie. Protein denaturation in intact hepatocytes and isolated cellular organelles during heat shock. *The Journal of cell biology*, 122(6):1267–1276, 1993.

[15] A. Lervik et al. Heat transfer in protein–water interfaces. *Physical Chemistry Chemical Physics*, 12(7):1610–1617, 2010.

[16] Z. Li and P. Srivastava. Heat-shock proteins. *Current protocols in immunology*, 58(1):A–1T, 2003.

[17] C. Liu, Z. Li, and Z. Zhang. Mechanisms of laser nanoparticle-based techniques for gene transfection—a calculation study. *Journal of biological physics*, 35:175–183, 2009.

[18] J. A. McCammon and S. C. Harvey. *Dynamics of proteins and nucleic acids*. Cambridge University Press, 1988.

[19] T. Nakano, A. W. Eckford, and T. Haraguchi. *Molecular communication*. Cambridge University Press, 2013.

[20] C. Nicolas Nicolaz et al. Absence of direct effect of low-power millimeter-wave radiation at 60.4 GHz on endoplasmic reticulum stress. *Cell biology and Toxicology*, 25:471–478, 2009.

[21] I. V. K. Reddy and J. M. Jornet. Multi-physics Analysis of Electromagnetic Wave Propagation and Photothermal Heating in Human Tissues at Terahertz and Optical Frequencies. In *2022 18th International Conference on Distributed Computing in Sensor Systems (DCOSS)*, pages 357–363. IEEE, 2022.

[22] C. B. Reid, G. Reese, A. P. Gibson, and V. P. Wallace. Terahertz time-domain spectroscopy of human blood. *IEEE Transactions on Terahertz Science and Technology*, 3(4):363–367, 2013.

[23] M. A. Schroer et al. Probing the existence of non-thermal Terahertz radiation induced changes of the protein solution structure. *Scientific Reports*, 11(1):22311, 2021.

[24] P. H. Siegel. Terahertz technology in biology and medicine. *IEEE transactions on microwave theory and techniques*, 52(10):2438–2447, 2004.

[25] A. K. Singh, L. L. McGoldrick, and A. I. Sobolevsky. Structure and gating mechanism of the transient receptor potential channel TRPV3. *Nature Structural & Molecular Biology*, 25(9):805–813, 2018.

[26] J.-H. Son. *Terahertz biomedical science and technology*. CRC Press, 2014.

[27] D. A. Turtton et al. Terahertz underdamped vibrational motion governs protein-ligand binding in solution. *Nature communications*, 5(1):1–6, 2014.

[28] N. Wright and J. Humphrey. Denaturation of collagen via heating: an irreversible rate process. *Annual review of biomedical engineering*, 4(1):109–128, 2002.

[29] C. Xie et al. Single pulse heating of a nanoparticle array for biological applications. *Nanoscale advances*, 4(9):2090–2097, 2022.

[30] J. Xu, K. W. Plaxco, and S. J. Allen. Probing the collective vibrational dynamics of a protein in liquid water by terahertz absorption spectroscopy. *protein Science*, 15(5):1175–1181, 2006.

[31] P.-H. Yang and J. A. Rupley. Protein-water interactions. Heat capacity of the lysozyme–water system. *Biochemistry*, 18(12):2654–2661, 1979.